INTERACTIVE ESTIMATION OF STRATAL CONTINUITY IN DEEP WATER SEQUENCES

INTERACTIVE ESTIMATION OF STRATAL CONTINUITY IN DEEP WATER SEQUENCES

D. BRADFORD MACURDA, JR.
The Energists
10260 Westheimer, Suite 300
Houston, Texas 77388

H. ROICE NELSON, JR. and KEVIN DONIHOO
Landmark Graphics Corporation
333 Cypress Run
Houston, Texas 77094

ABSTRACT

The basic unit of analysis in seismic stratigraphy is the sequence. The continuity of reflectors within the sequence is used as an indicator of environmental homogeneity or heterogeneity. At a gross scale, this provides some indication of the continuity of bedding plane surfaces. Most seismic facies studies do not quantify the three-dimensional extent of individual reflectors. If the extent is measured, it places upper limits on the possible continuity of strata and the reliability of correlations of smaller scale units as beds and bed sets.

The Porcupine Basin off southwestern Ireland was formed in the Cretaceous. Subsidence during the Tertiary was such that present-day sediments are being deposited in over 1000 meters of water. Seismic data show the Miocene-Pleistocene fill to be composed of nine seismic sequences deposited in deep water environments. The genetic units are inferred to include erosional channels, levees, submarine fans, contourites, and basin plain deposits. Measurement of the continuity of individual reflectors in each of these sedimentary units suggests the homogeneity or heterogeneity of the deposits. The length of the reflectors in deposits of each of the units belonging to a specific sedimentary environment matches with geological expectations. These data can be used to estimate the distances over which detailed correlations (e.g., wells) can be expected to be reliably made.

INTRODUCTION

One of the most perplexing and important problems facing geologists is to predict stratal continuity. Continuity is extremely important to reservoir geologists and engineers who must produce the hydrocarbon from the reservoirs or conduct secondary recovery operations. How far does a bed, a bed set, or parasequence extend? The answers to such questions are usually indeterminate. A well bore is only a few centimeters wide and extrapolation away from it is based largely upon concepts or models. Outcrops are usually limited in size. Continuity establishes the fine-scale correlation of stratigraphic units; these are below the levels of biostratigraphic resolution. Stratal continuity reflects the homogeneity or heterogeneity of environmental processes.

Data on stratal continuity in three dimensions are limited. Therefore we attempted to experiment at a scale larger than that of bed or bed set, by trying to estimate the stratal continuity of sediments in a deep-water setting using seismic data. The concept is that one can subdivide the sediments into a series of sequences in the seismic section. Then, using seismic facies analysis and external geometry, one can work out the environmental setting or settings within the sequence. Next one measures the lengths of individual reflectors in each environmental setting and compares these lengths to one another. Since reflectors within a sequence are composite images of bedding plane configurations, then the statistics on reflection continuity in the seismic data can provide a coarse scale estimate of stratal continuity. This provides a measure of the reliability of correlations of stratigraphic sections in different environmental settings.

In order for the proposed procedure to have any validity or opportunity for success, several prerequisites relevant to acquisition and processing must apply: a) the data must be of good quality; b) the strata must not have suffered extensive tectonic deformation; c) the data should have a high frequency component; d) the use of smoothing functions such as trace averaging should be minimized and e) the data examined should all be from the same survey.

THE SETTING

The seismic data on the deep-water sediments which we examined come from the Porcupine Basin, southwest of the Republic of Ireland (Figure l). The Porcupine Basin underwent extensional rifting in the earliest Cretaceous; thereafter passive subsidence resulted in a basin which has been partially infilled with a maximum of 7-8 km of sediments (Masson and Miles, 1986). Gravity data show the basin's extent (Figure 2). The north-central part of the basin subsided into the bathyal zone in the Eocene; it has not been uplifted since (Naylor and Shannon, 1982; Macurda, 1986: Crocker and Shannon, 1987). The units we examined are imaged on seismic sections from the seafloor downward for 1.3-1.5 seconds (two-way travel time) (Figures 3 and 4). Present water depths, in the area examined, range from 500 to over 1,500 m (Figure 5). Geologically, these units are Miocene and younger in age. They are composed of fine grained siliciclastics in wells drilled north of the study area. The seismic data were acquired as part of a speculative survey in 1981 by Merlin Geophysical. The data were shot with a wide airgun array with a shot point interval of 25m. They were recorded at 60 fold with a 4ms sample rate; the low cut and high cut filters were 8 and 90 hz. The data were processed at 30 fold by using a two shot vertical sum. They were deconvolved before and after stack. The data are minimum phase. A two dimensional filter was used for dip rejection. The data are migrated and the automatic gain controls operator was short. A time variant filter resulted in a frequency range of 8 or 12 to 50 or 55 hz in the interval examined.

The study interval is composed of two major depositional units or megasequences (Figure 6). The lower one (Megasequence 2) is composed of sediments deposited by contourites in the eastern part of the basin, grading into bathyal basin plain deposits to the west. The upper unit (Megasequence 1) is composed of sediments associated with submarine fans, slides, basin plain and onlap fill deposits. A general discussion of facies models and depositional processes for deep-water fine-grained sediments was presented by Stow and Piper (1984); reference should be made to this publication for illustrations of typical sedimentary facies and successions in these environments.

The lower megasequence was divided into three sequences, the upper into six. The environments within each sequence were inferred using reflection configurations and external geometry.

DATA ANALYSIS

Megasequence 2 is dominated by a series of steeply inclined reflectors in the eastern part of the basin. Mapping of these suggests they were produced by contour currents whose direction of flow was from north-northwest to south-southeast (Macurda and Nelson, 1989). The contourite facies is illustrated in Figure 7; the steeply inclined reflectors were measured using a Landmark workstation, in which the horizontal scale is displayed for the interval chosen. Immediately west of the steeply inclined reflectors of the prograding portion of the contourite drift is a channel flanked by a levee. The levee facies is displayed in Figure 8. The levee facies was distinguished by its external geometry and discontinuous pattern; flat, basin-plain deposits are found toward the basin centre. The other reflectors measured in the upper portion of Megasequence 2 are associated with a large submarine slide formed in the western part of the basin. Rotation of the reflectors in this mass movement is illustrated in Figure 9. The component measured involves the rotated reflectors associated with the listric fault.

A submarine fan is developed in the west-central portion of the basin in Megasequence 1. The upper part is associated with a proximal setting, the lower portion with a medial setting. The two facies are illustrated in Figures 10 and 11, as are examples of the reflectors measured. Various types of channel fill deposits are also associated with Megasequence 1 (Figure 12). Some are found in the proximal fan whilst others are fills of erosional canyons associated with sequence boundaries in other environments.

Three other environments were recognized. These include basin plain or overbank deposits, found in both Megasequences 1 and 2 (Figure 13) and onlap fill deposits on both margins of the basin in Megasequence 1 (Figure 14). Subsequent to the deposition of Megasequence 1, there is inferred to have been extensive dewatering which affected the continuity of the strata; this can be seen as the offset reflectors in Figure 15. The loss of continuity is diagenetic and would clearly influence reservoir behavior.

THE RESULTS

We attempted to make at least twenty measurements at random of the length of the reflectors in each facies. This was not always possible because of an inadequate sample size. After the measurements were accumulated, they were transferred to an X,Y,Z file where the data could be evaluated with a standard spread-sheet program; in our case we used Excel on a Mac II personal computer. The figures presented here are from the Excel graphics package. The first stage was to build a table of reflection lengths. We used bar graph displays to provide comparative visual estimates of reflection length. A formal statistical analysis of the data has not been attempted yet; therefore, the following comments are a qualitative analysis of the data.

For the contourite facies (Figure 7), there is a large variance, with reflection length varying from less than 600 m to over 6,000 m. The distribution appears to be bimodal, with principal lengths clustering near 1,000 and 4,000 m. For the levees (Figure 8) the coefficient of variation is lower; reflection continuity varies from 2,000 to 4,500 m. The reflectors in the submarine slide flow (Figure 9) are, as expected, mostly short (less than 400 m), although a few extended to 7,000 m.

Reflectors in the proximal fan (Figure 10) are longer than those of the contourite, levee, or submarine slide environments. The mean value picked was about 6,000 m and some extend up to 16,000 m. The reflectors of the medial fan (Figure 11) do not vary much in length from those of the proximal fan. They range from 3,000 to 15,000 m, with most being near 6,000 m in length. The channel fill deposits (Figure 12) are short; most fall between 1,000 and 4,000 m. The reflectors of the basin plain or overbank deposits (Figure 13) are, as would be expected, the longest of all the continuous reflectors we measured. These varied from 10,000 m to in excess of 60,000 m. The reflectors of the onlap fill deposits (Figure 14) are shorter, between 2,000 and 14,000 m in length. The strata most extensively effected by dewatering are the basin plain or overbank deposits (Figure 15). Here stratal continuity has been severely affected, with reflectors varying from less than 500 m to over 3,000 m; most measurements were 500 m or less.

When all of the data are displayed simultaneously, the basin plain or overbank deposits produce a highly asymmetrical bar graph. Figure 16 shows the average length of reflectors for each of the depositional environments. Removal of this environment and rescaling of the data brings out another cluster of reflectors, which include the reflectors of the proximal and medial fan and the onlap fill deposits (Figure 17). By removing these and rescaling the data again, the third cluster emerges, which includes the reflectors of the gravity slide deposits, contourites, levees, and channel fills. The dewatered strata form a fourth cluster, shorter than any of the others.

CONCLUSIONS

Our attempt at using reflection length as a large scale measure of bedding continuity must be regarded as a pilot project. Many questions can be posed about the data, its environmental interpretation, and exactly how the measurements should be made. Ideally, it should involve a 3d survey in which the entire reflector can be traced in 3 dimensions. Despite such possible qualifications, we are encouraged by the results. The variations in the length of the reflectors between different environments agrees with our intuitive geological expectations. Four clusters appear to be present, and those reflection lengths which are expected to be the longest and shortest are found to be so. We suggest the technique can be refined and exploited in environments other than deep-water sediments. The most rigorous test would be a 3d survey of a producing field with closely spaced wells.

Measuring the length of the reflectors establishes limits on the continuity of finer scale units, such as beds and bed sets, suggests refinements in fine-scale correlations in different environments, and aids understanding of the homogeneity or heterogeneity of environments from both a genetic and reservoir management perspective.

ACKNOWLEDGMENTS

We are indebted to Merlin Geophysical for making available to us the data which we analyzed in this study and to Landmark Graphics for the use of a workstation to conduct the analysis. This paper was presented as an interactive poster paper at the Norwegian Petroleum Society's Conference: Correlation in Hydrocarbon Exploration, Bergen, Norway, 3-5 October, 1988.

REFERENCES

Crocker, P.E., and Shannon, P.M., 1987, The evolution and hydrocarbon prospectivity of the Porcupine Basin, offshore Ireland, J. Brooks and K. W. Glennie, (eds.), Petroleum geology of northwest Europe, Graham and Trotman, v. 2, p. 633-642.

Macurda, D.B., Jr., 1986, Sedimentary fill and stratigraphic traps of Porcupine Basin, offshore Ireland: Abs., AAPG Bull., v. 70, no. 5, p. 614.

Macurda, D.B., Jr. and Nelson, H. R., Jr., 1989, Interactive Interpretation of Morphology of Upper Tertiary Contourites, Porcupine Basin, Ireland: AAPG Bull., v. 73, p. 384.

Masson, D. G., and Miles, P.R., 1986, Structureand development of Porcupine Seabight sedimentary basin, offshore southwest Ireland: AAPG Bull., v. 70, no. 5, p. 536-348.

Naylor, D., and Shannon, P.M., 1982, Geology of offshore Ireland and west Britian: London, Graham and Trotman, p. 161.

Stow, D.A.V., and Piper, (eds.), D.J.W., 1984, Deep-water fine-grained sediments: facies models in D.A.V. Stow and D.J.W. Piper (eds.), Fine-Grained Sediments: Deep-Water Processes and Facies: Geol. Soc. Spec. Pub., no. 15, p. 611-646.

FIGURE LEGENDS

Figure 1. Location of the Porcupine Basin, southwest of Ireland.

Figure 2. Digitized gravity map of the Porcupine Basin, after Masson and Miles (1986).

Figure 3. Seismic line showing the shallow sequences on the west edge of Porcupine Basin. Black represents a peak while gray represents a trough. Vertical scale is in milliseconds, two way travel time.

Figure 4. Seismic line showing the shallow sequences on the east edge of the Porcupine Basin. Black represents a peak while gray represents a trough. Vertical scale is in milliseconds, two way travel time.

Figure 5. Regional east-west seismic line across Porcupine Basin. Vertical scale is in milliseconds, two way travel time.

Figure 6. Regional east-west seismic line across the Porcupine Basin illustrating the bed length of different facies measured. Individual measurements illustrated in Figures 7 through 15.

Figure 7. Illustration and measurement of the contourite facies in Sequence 2a. Data with superimposed sequence boundaries and measured reflectors in lower part of figure. Sequence boundaries and measured reflectors abstracted in upper part of figure. Vertical scale is two way travel time. Horizontal scale given in meters in lower part of figure.

Figure 8. Illustration and measurement of the levee facies in Sequence 2. See Figure 7 for explanation of symbols.

Figure 9. Illustration and measurement of the submarine slide facies in sequences 1c, 1d, and 1e. See Figure 7 for explanation of ` symbols.

Figure 10. Illustration and measurement of the proximal submarine fan facies in Sequence 1c. See Figure 7 for explanation of symbols.

Figure 11. Illustration and measurement of the medial submarine fan facies in Sequence 1d. See Figure 7 for explanation of symbols.

Figure 12. Illustration and measurement of the channel fill facies in sequences 1c, 1d, 1e and 2. See Figure 7 for explanation of symbols.

Figure 13. Illustration and measurement of the basin plain - overbank facies in Sequence 1e and Sequence 2. Note that the seismic section has been flattened on the top of Sequence 2a. See Figure 7 for explanation of symbols.

Figure 14. Illustration and measurement of the onlap fill facies beneath the top of Sequence 1d. See Figure 7 for explanation of symbols.

Figure 15. Illustration and measurement of the dewatered facies in Megasequence 1. See Figure 7 for explanation of symbols.

Figure 16. Average reflection lengths of all the environmental facies.

Figure 17. Composite graphical summary of the reflection lengths with the basin-plain/overbank facies removed.

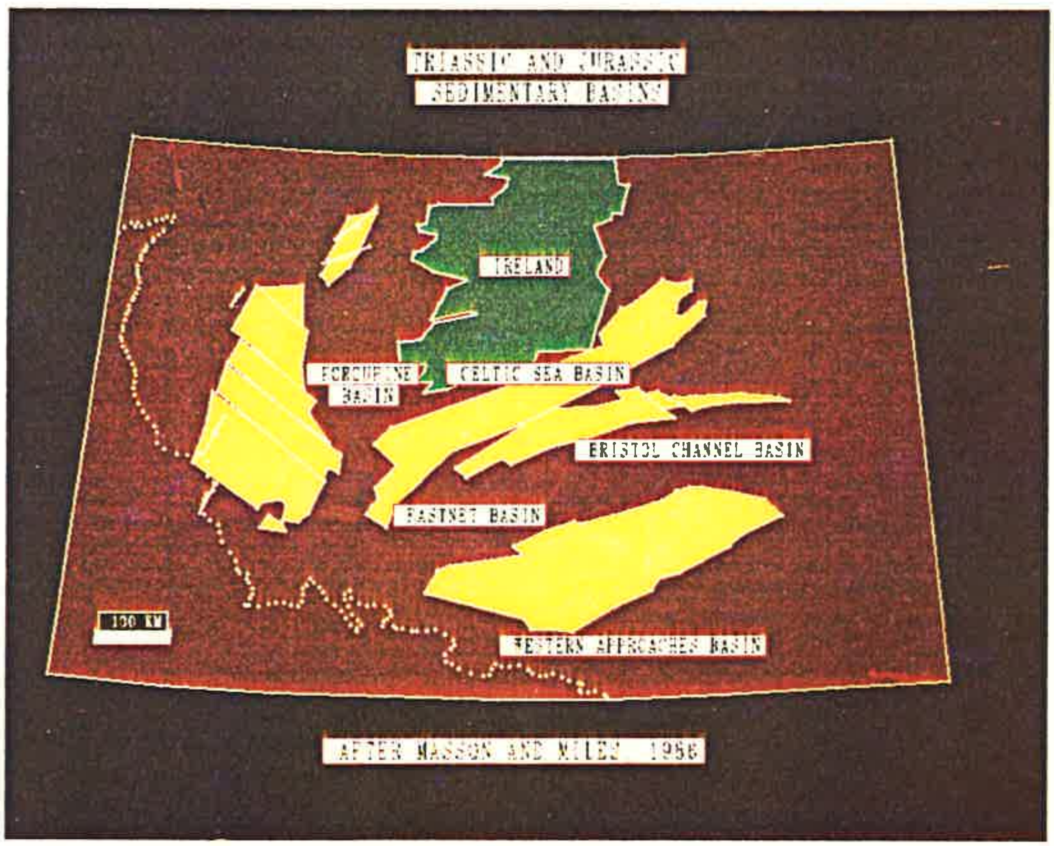

Figure 1

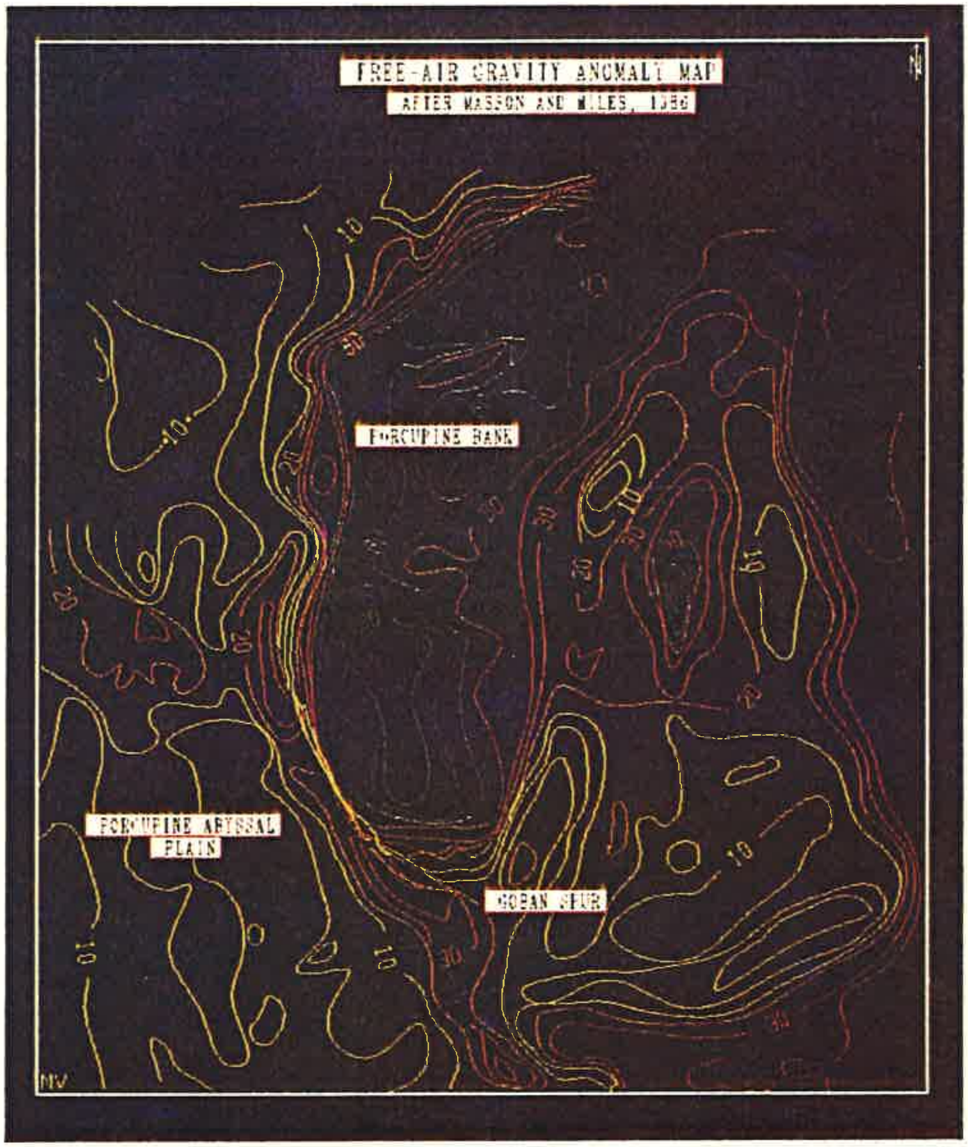
FREE-AIR GRAVITY ANOMALY MAP
AFTER MASSON AND MILES, 1986
PORCUPINE BANK
PORCUPINE ABYSSAL PLAIN
GOBAN SPUR

Figure 2

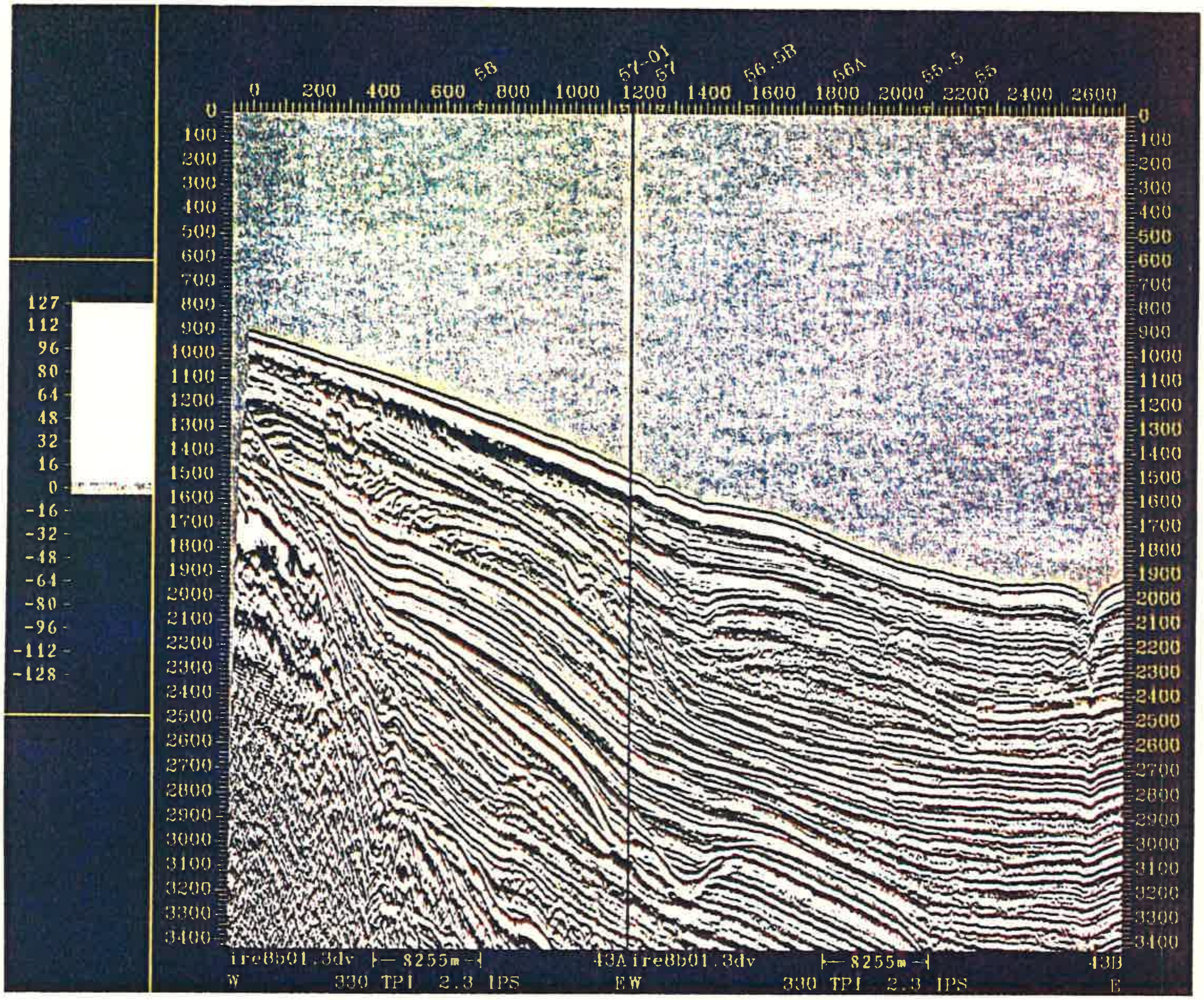
0 200 400 600 800 1000 1200 1400 1600 1800 2000 2200 2400 2600
58 57-01 57 56.5B 56A 55.5 55
127 112 96 80 64 48 32 16 0 -16 -32 -48 -64 -80 -96 -112 -128
ire8b01.3dv ⊢ 8255m ⊣ 43A ire8b01.3dv ⊢ 8255m ⊣ 43B
W 330 TPI 2.3 IPS EW 330 TPI 2.3 IPS E

Figure 3

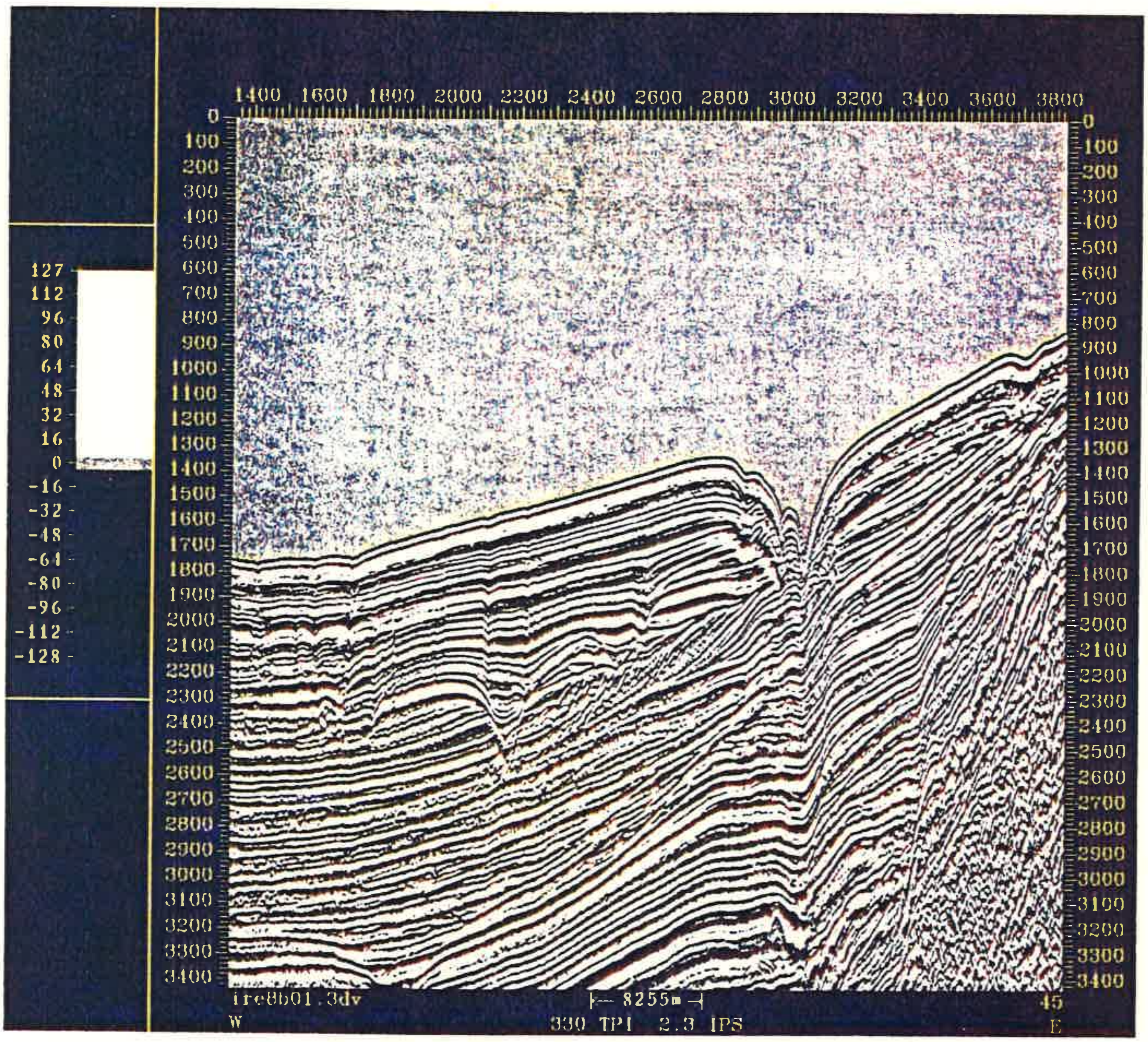
1400 1600 1800 2000 2200 2400 2600 2800 3000 3200 3400 3600 3800
127 112 96 80 64 48 32 16 0 -16 -32 -48 -64 -80 -96 -112 -128
0 100 200 300 400 500 600 700 800 900 1000 1100 1200 1300 1400 1500 1600 1700 1800 1900 2000 2100 2200 2300 2400 2500 2600 2700 2800 2900 3000 3100 3200 3300 3400
ire8b01.3dv
8255m
330 TPI 2.3 IPS
W
45
E

Figure4

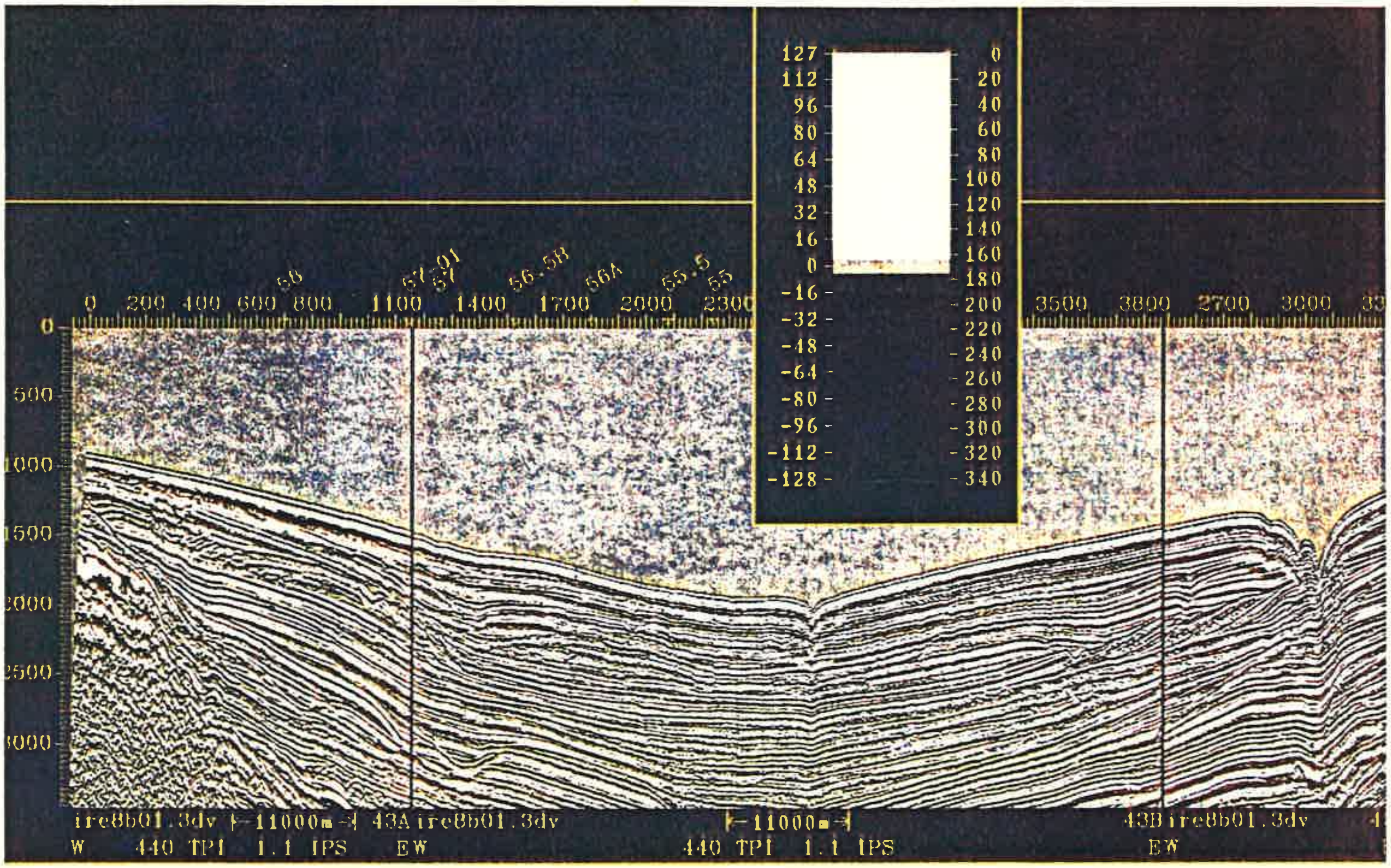
0 200 400 600 800 1100 1400 1700 2000 2300
3500 3800 2700 3000
68 67-01 67 66-5B 66A 65-5 65
0 500 1000 1500 2000 2500 3000
127 112 96 80 64 48 32 16 0 -16 -32 -48 -64 -80 -96 -112 -128
0 20 40 60 80 100 120 140 160 180 200 220 240 260 280 300 320 340
ire8b01.3dv |-11000m-| 43A ire8b01.3dv
W 440 TPI 1.1 IPS EW
|-11000m-|
440 TPI 1.1 IPS
43B ire8b01.3dv
EW

Figure5

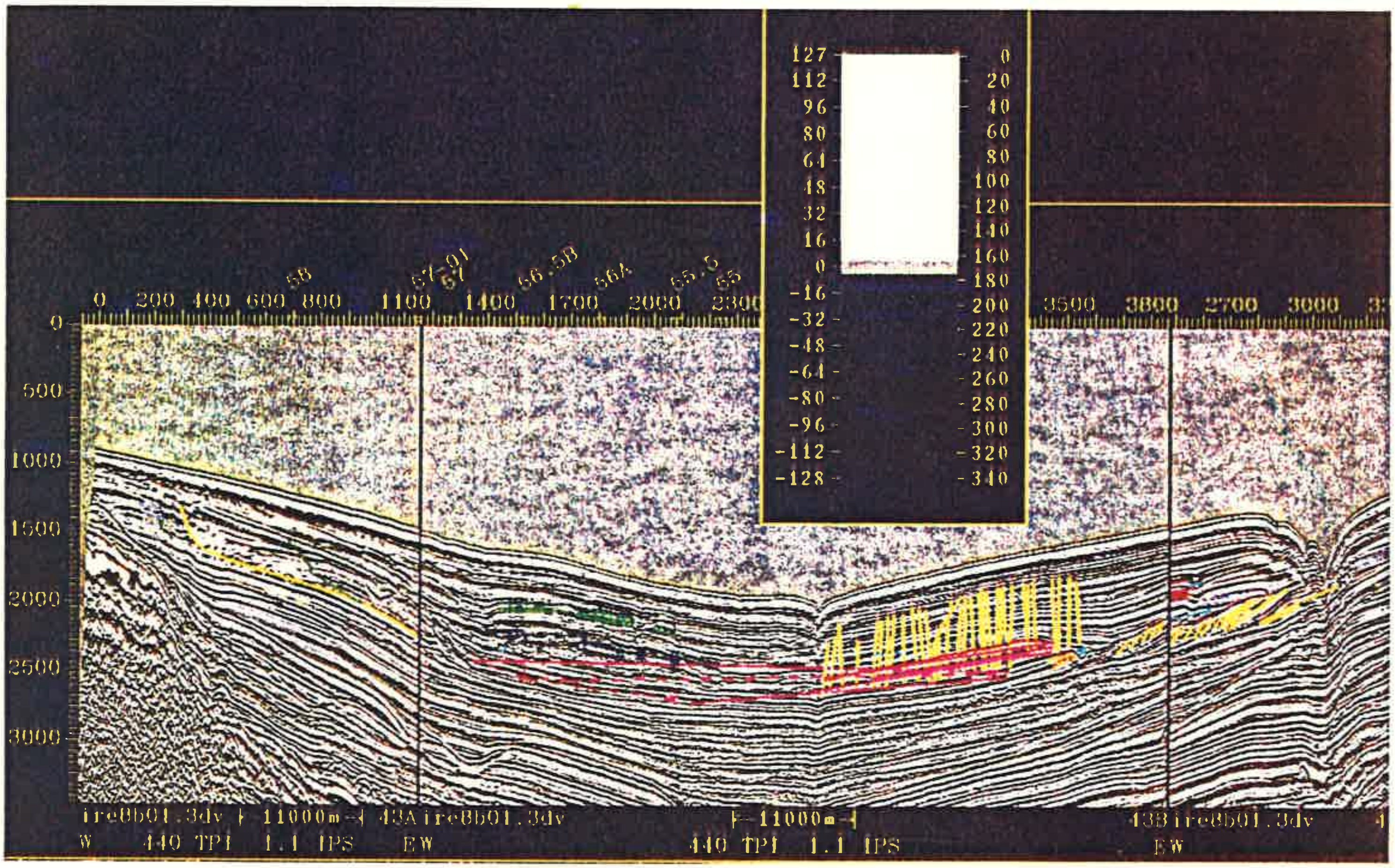

ire8b01.3dv ⊢ 11000m ⊣ 43A ire8b01.3dv
W 440 TPI 1.1 IPS EW
⊢ 11000m ⊣
440 TPI 1.1 IPS
43B ire8b01.3dv
EW

Figure 6

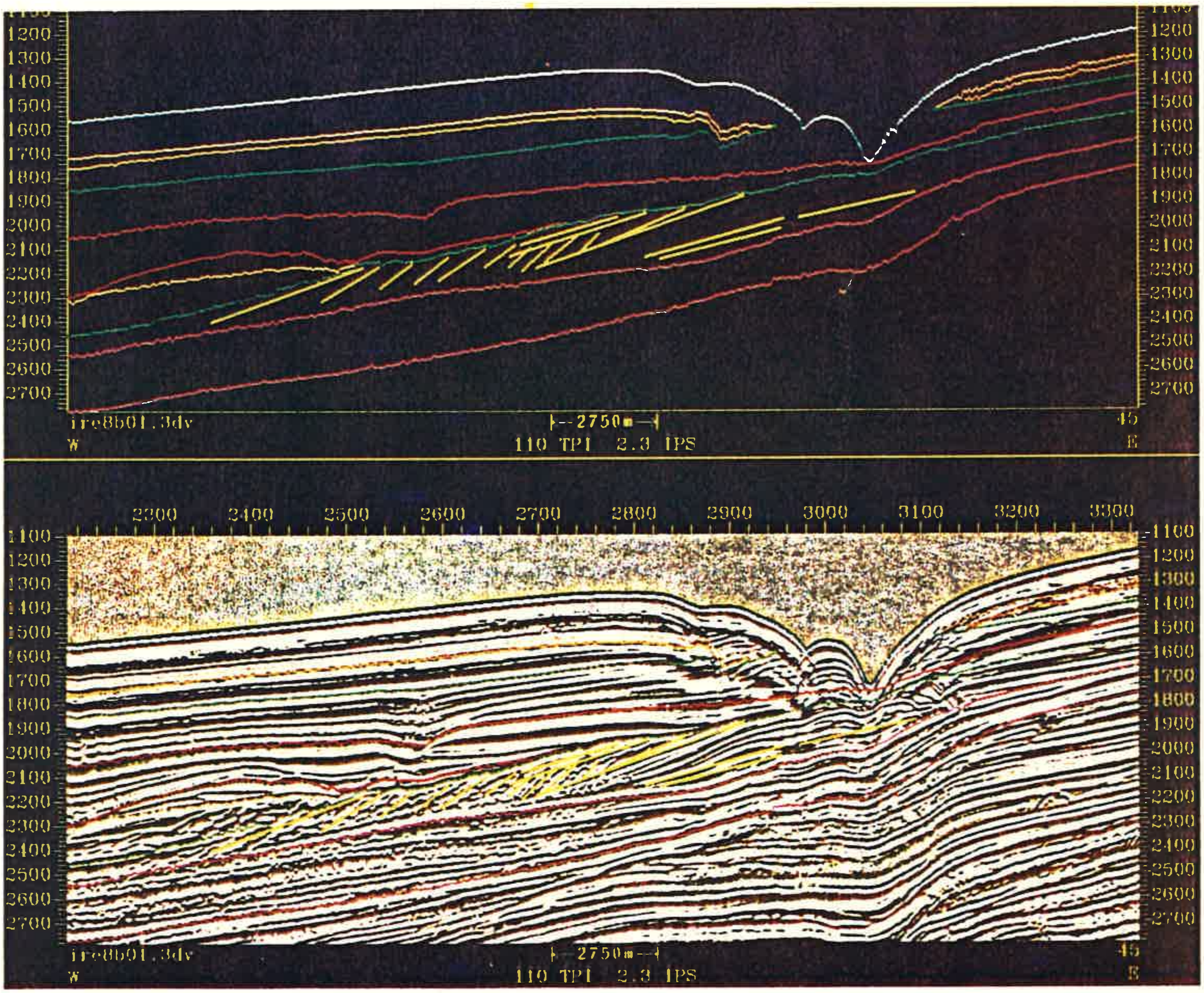
ire8b01.3dv
W
110 TPI 2.3 IPS
45
E
ire8b01.3dv
W
110 TPI 2.3 IPS
45
E

Figure7

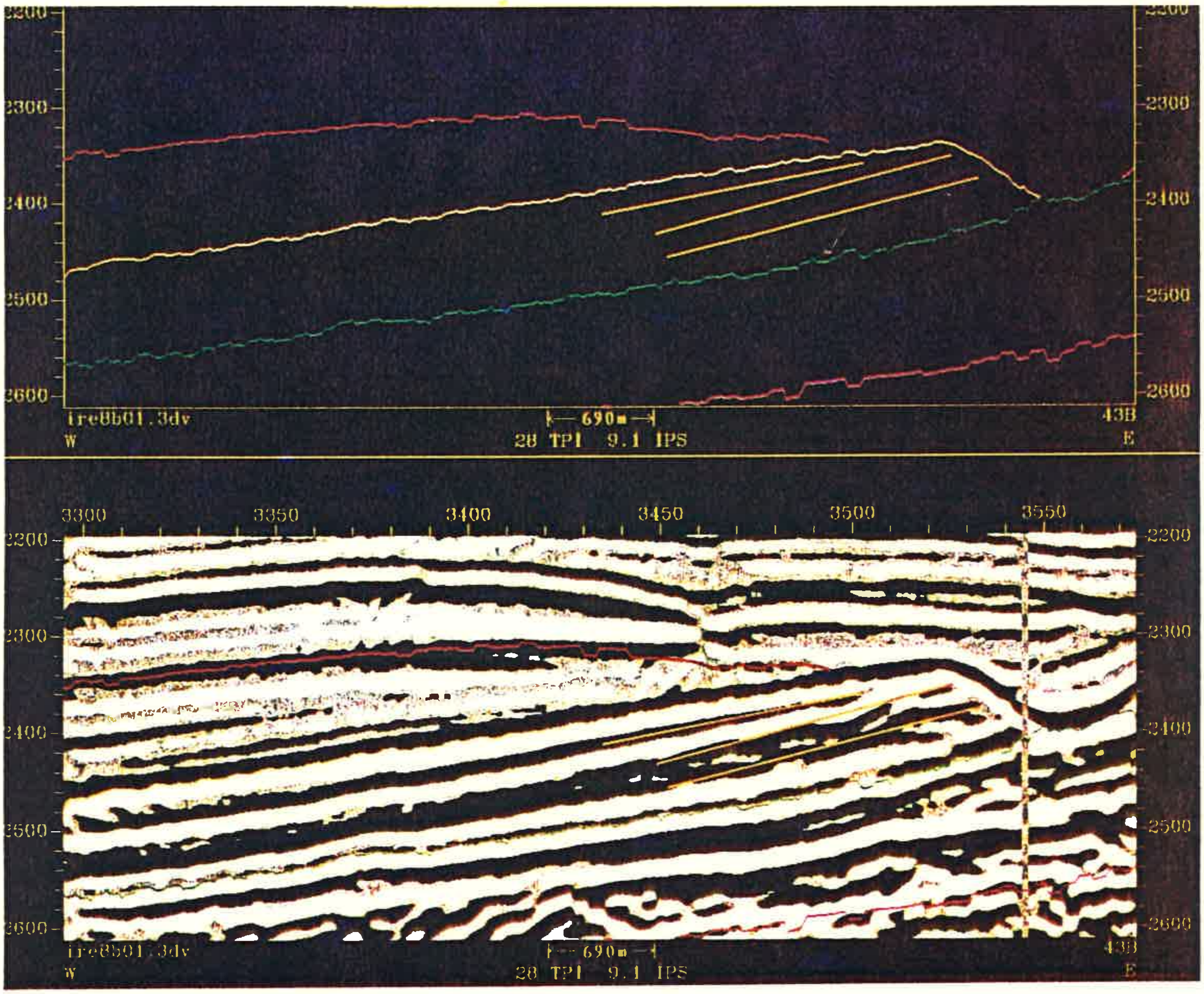

2200
2300
2400
2500
2600
ire8b01.3dv
690m
43B
W
E
28 TPI 9.1 IPS
3300
3350
3400
3450
3500
3550

Figure8

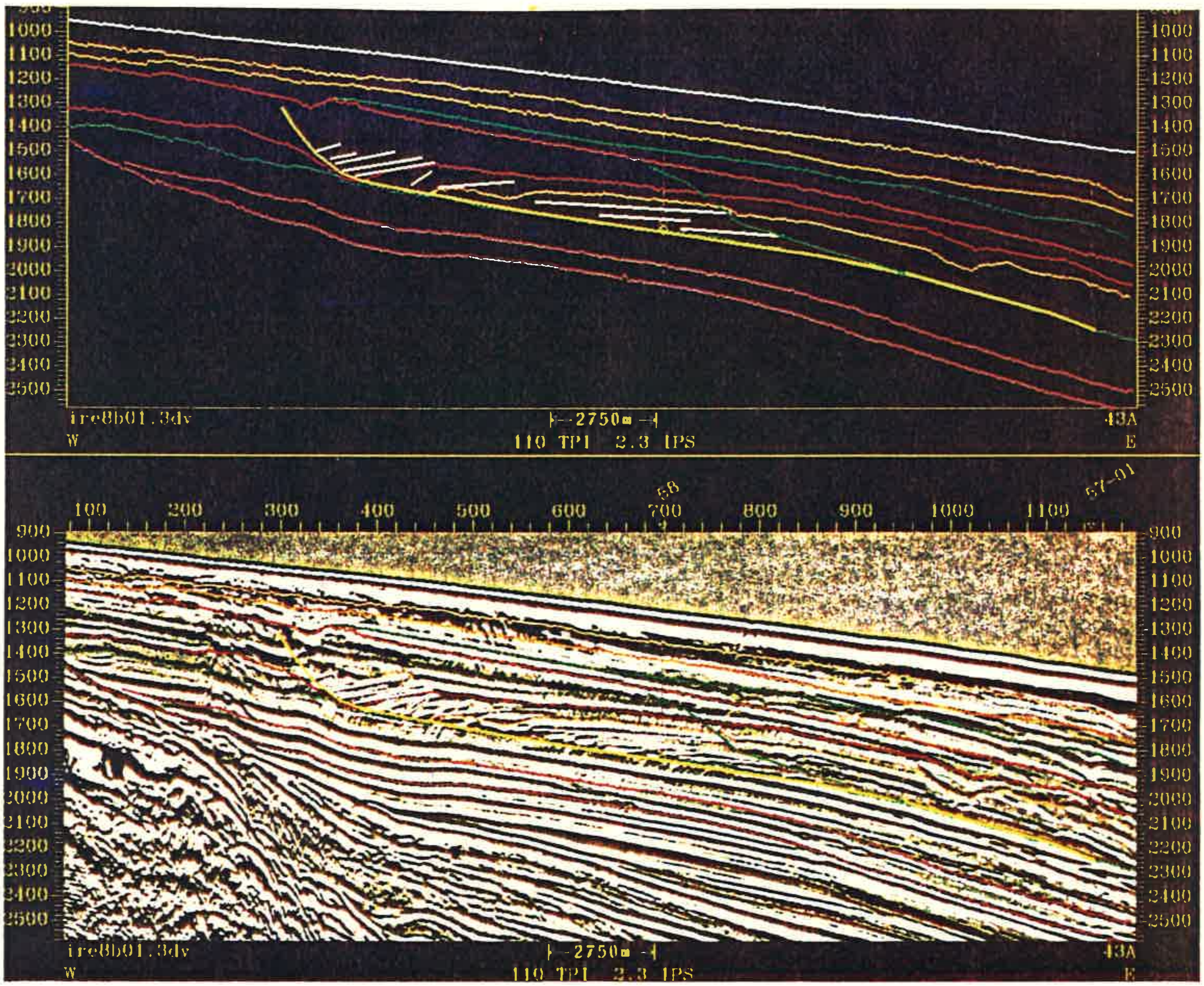
1000
1100
1200
1300
1400
1500
1600
1700
1800
1900
2000
2100
2200
2300
2400
2500
ire8b01.3dv
W
|--2750m--|
110 TP1 2.3 IPS
43A
E
100
200
300
400
500
600
700
800
900
1000
1100
900
ire8b01.3dv
W
|--2750m--|
110 TP1 2.3 IPS
43A
E

Figure9

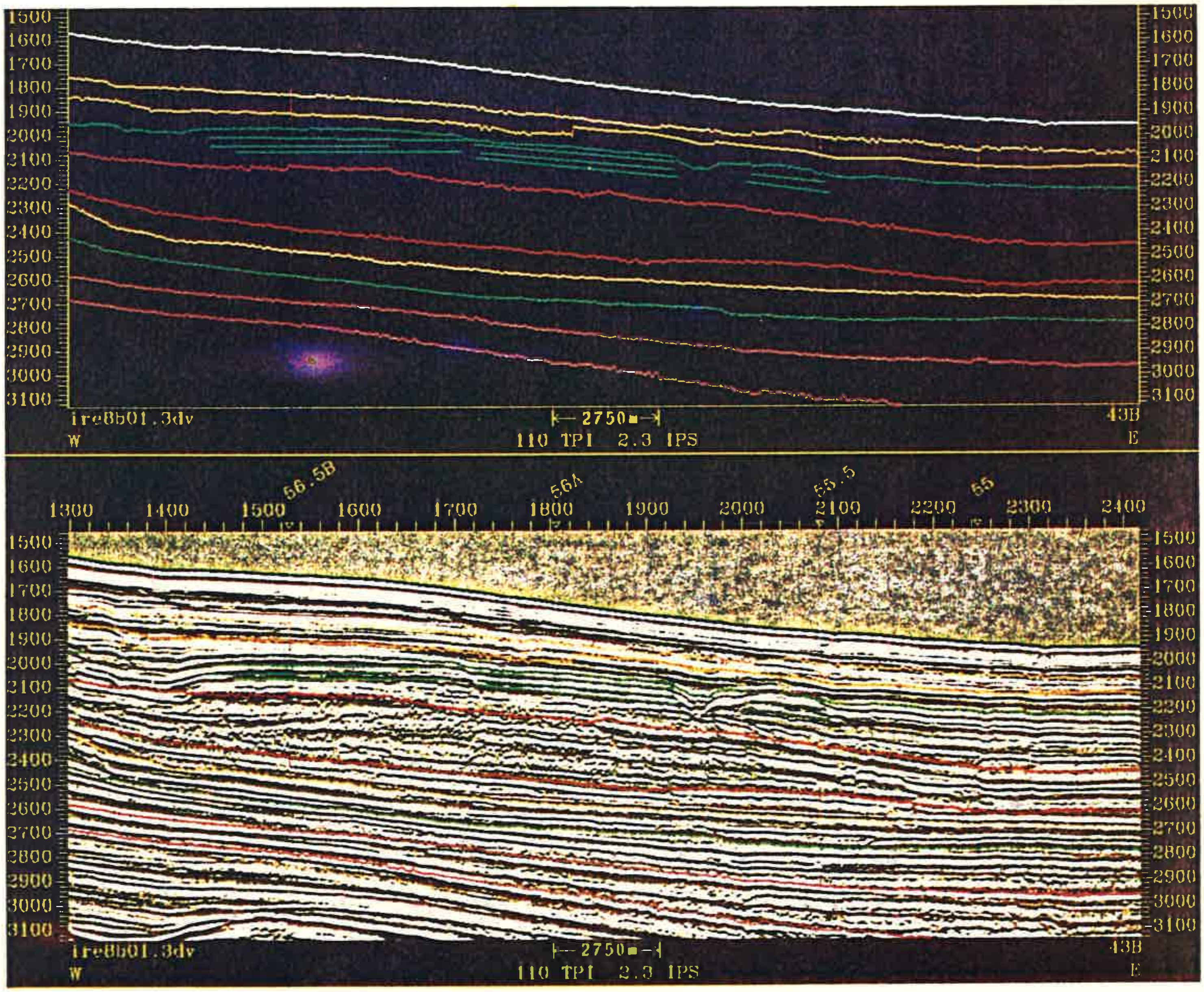
1500
1600
1700
1800
1900
2000
2100
2200
2300
2400
2500
2600
2700
2800
2900
3000
3100
ire8601.3dv
W
2750m
110 TPI 2.3 IPS
43B
E
56.5B
56A
55.5
55
1300
1400
1500
1600
1700
1800
1900
2000
2100
2200
2300
2400

Figure 10

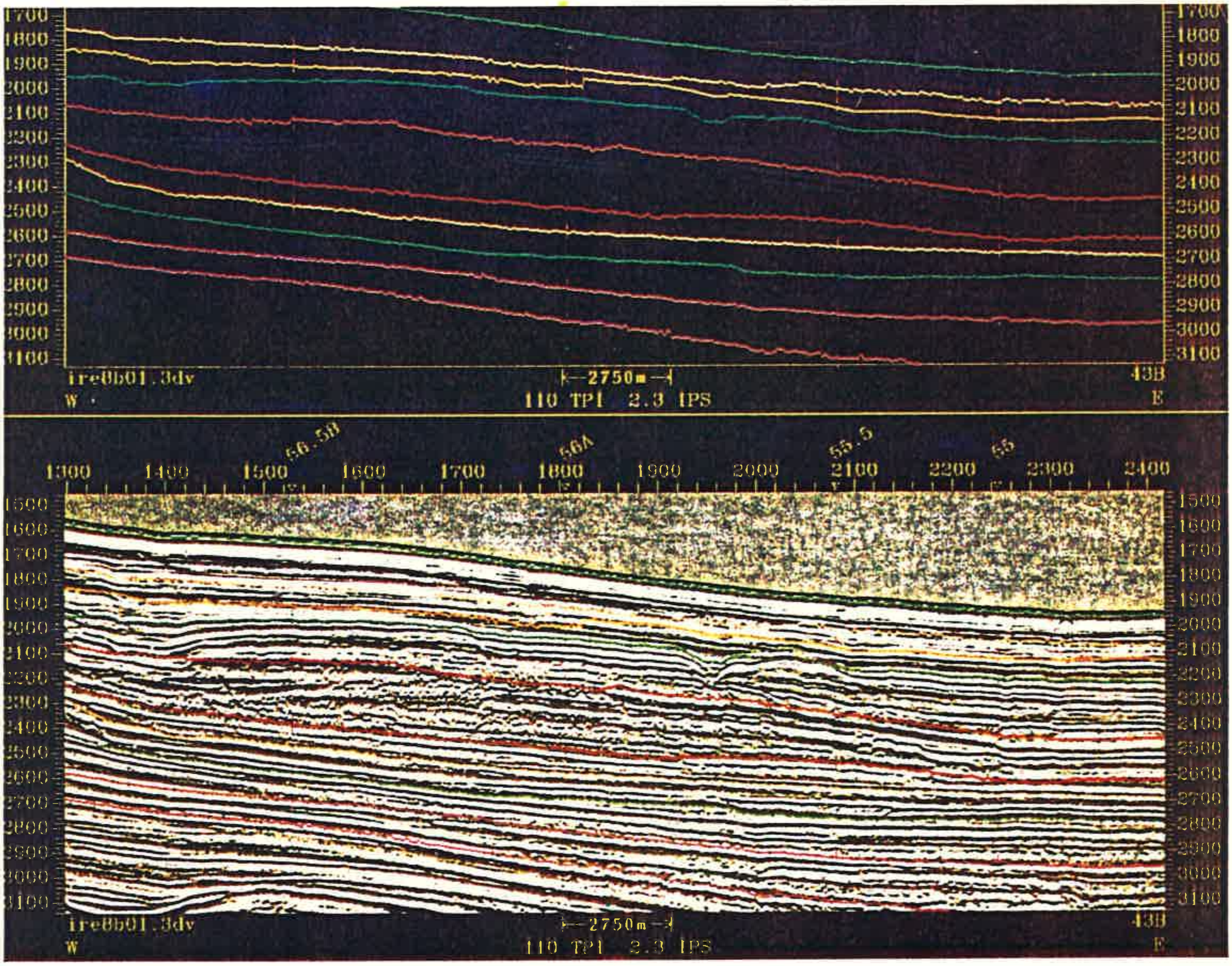

Figure 11

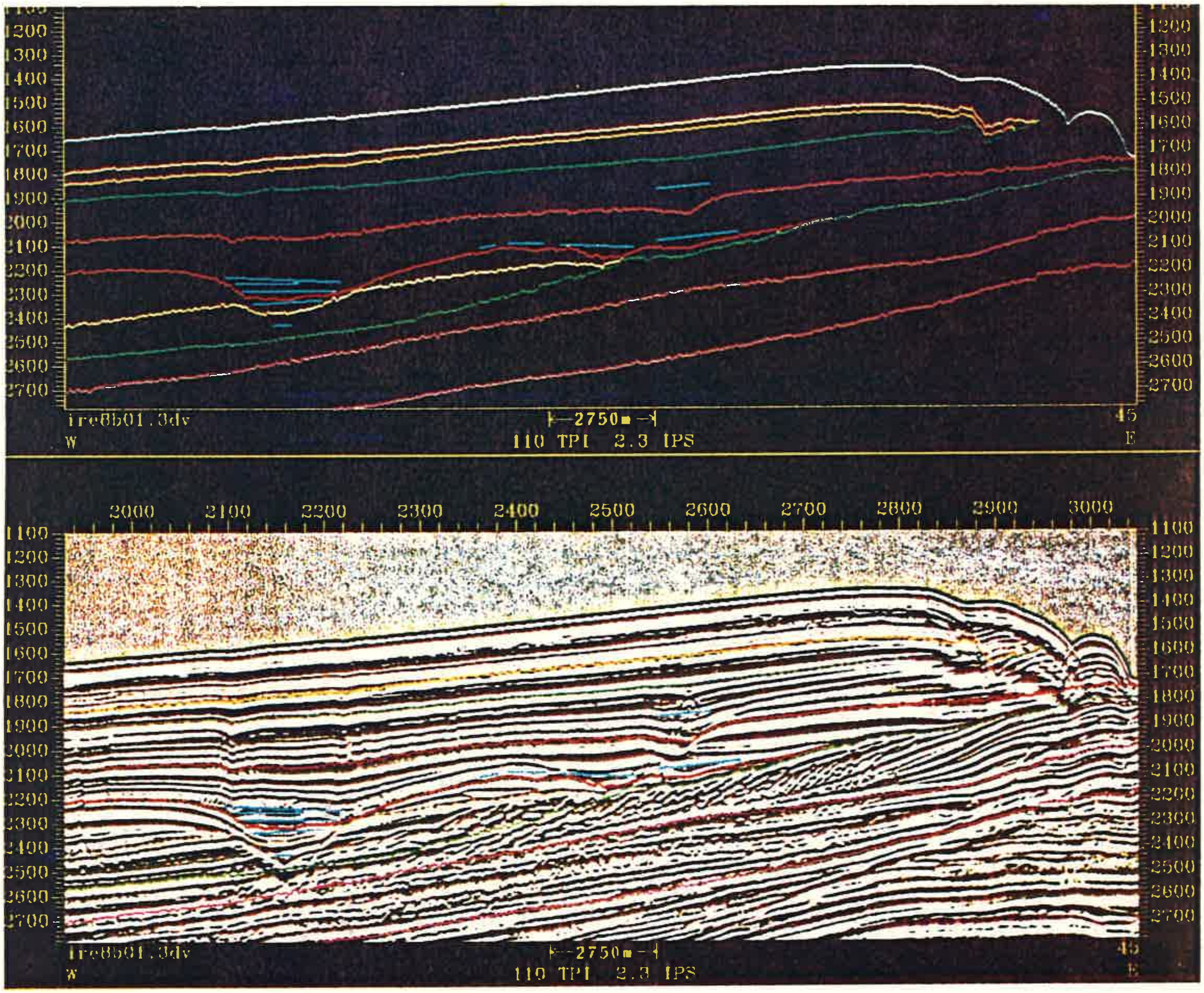
ire8b01.3dv
W
|--2750m--|
110 TPI 2.3 IPS
45
E
2000
2100
2200
2300
2400
2500
2600
2700
2800
2900
3000
ire8b01.3dv
W
|--2750m--|
110 TPI 2.3 IPS
45
E

Figure 12

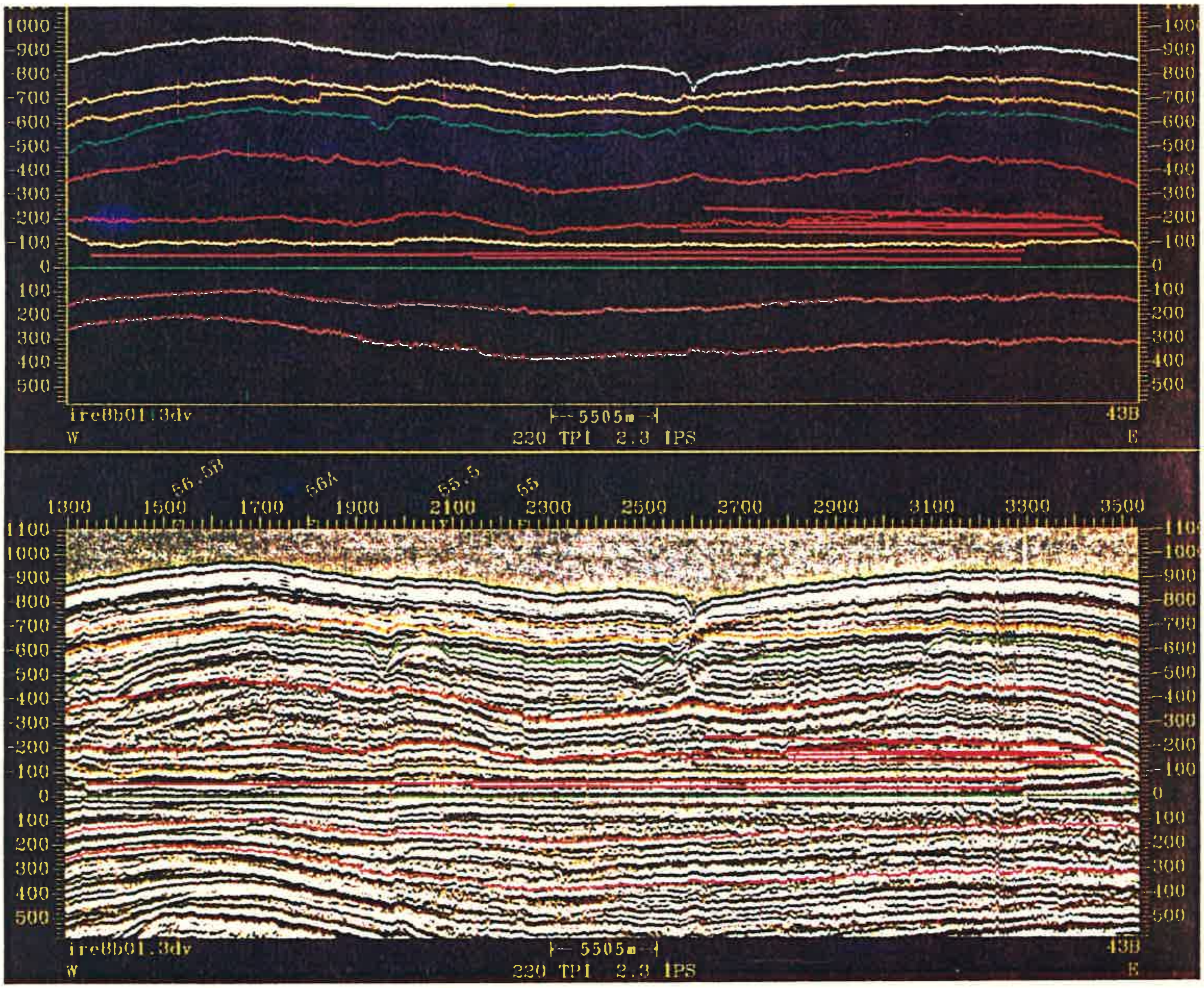
1000
900
800
700
600
500
400
300
200
100
0
100
200
300
400
500
ire8b01.3dv
5505m
43B
W
220 TPI 2.3 IPS
E
56.5B
56A
55.5
55
1300
1500
1700
1900
2100
2300
2500
2700
2900
3100
3300
3500
1100
ire8b01.3dv
5505m
43B
W
220 TPI 2.3 IPS
E

Figure 13

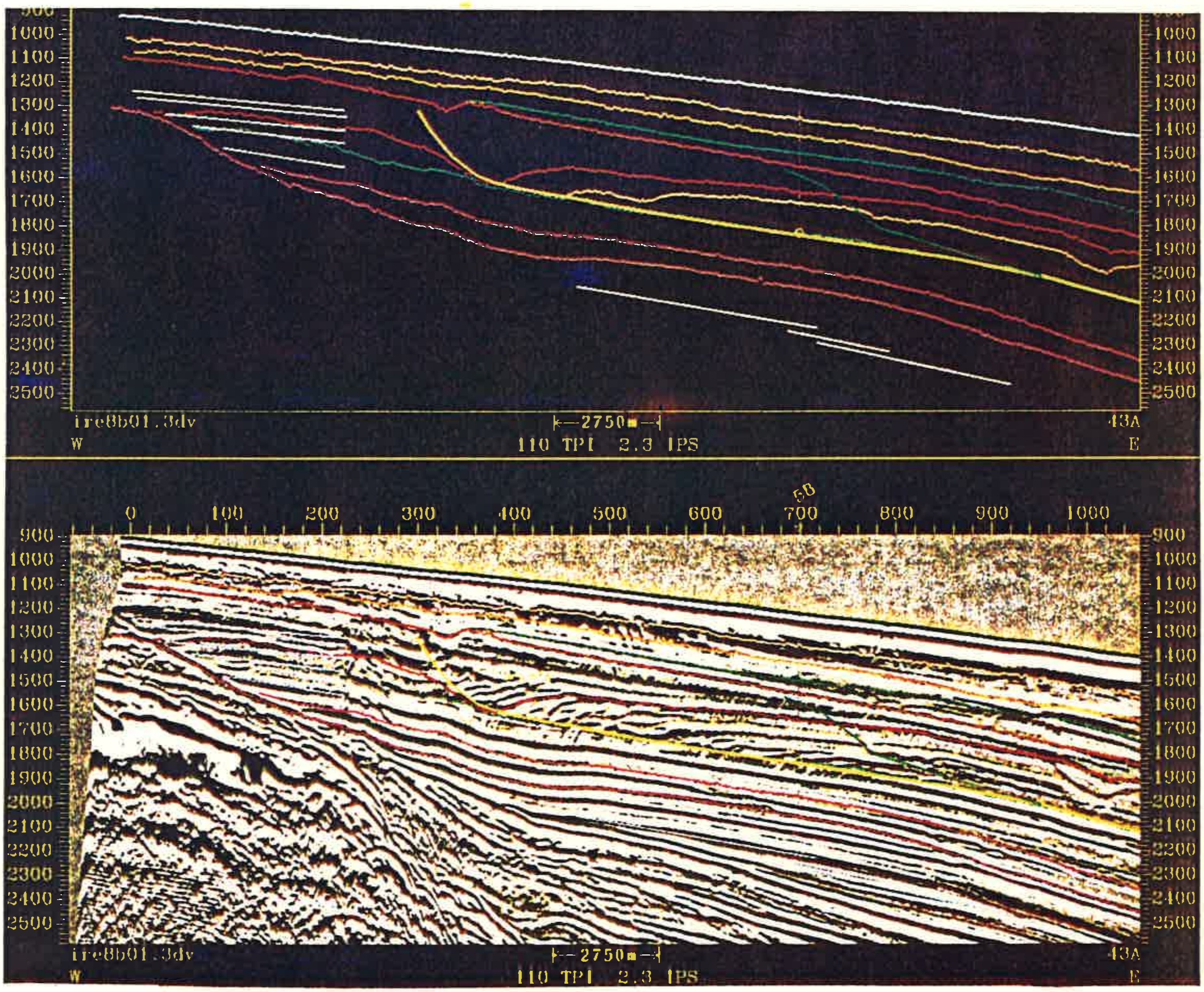
1000
1100
1200
1300
1400
1500
1600
1700
1800
1900
2000
2100
2200
2300
2400
2500
ire8b01.3dv
2750m
43A
W
110 TPI 2.3 IPS
E
0
100
200
300
400
500
600
700
800
900
1000
900
ire8b01.3dv
2750m
43A
W
110 TPI 2.3 IPS
E

Figure 14

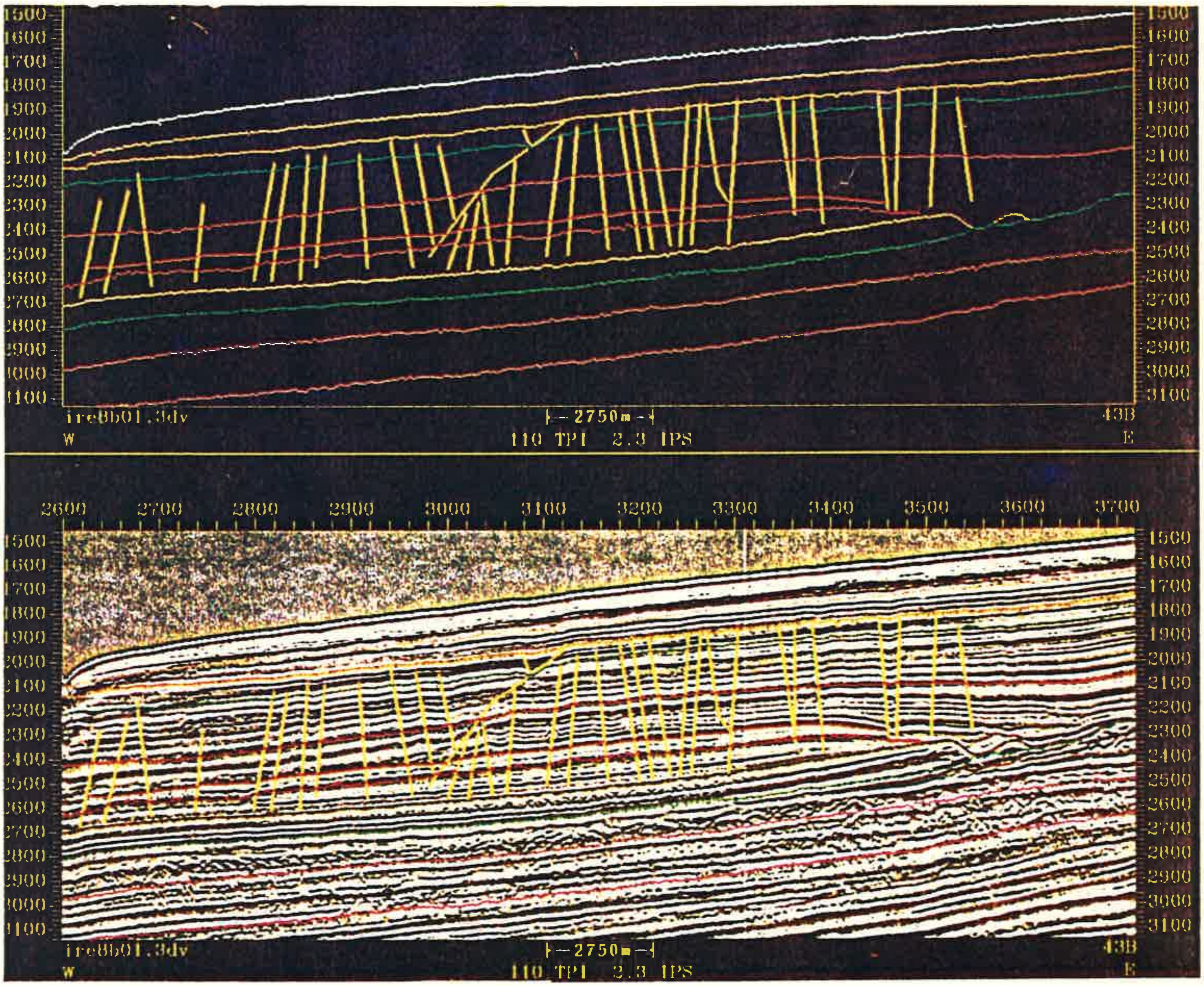

Figure 15

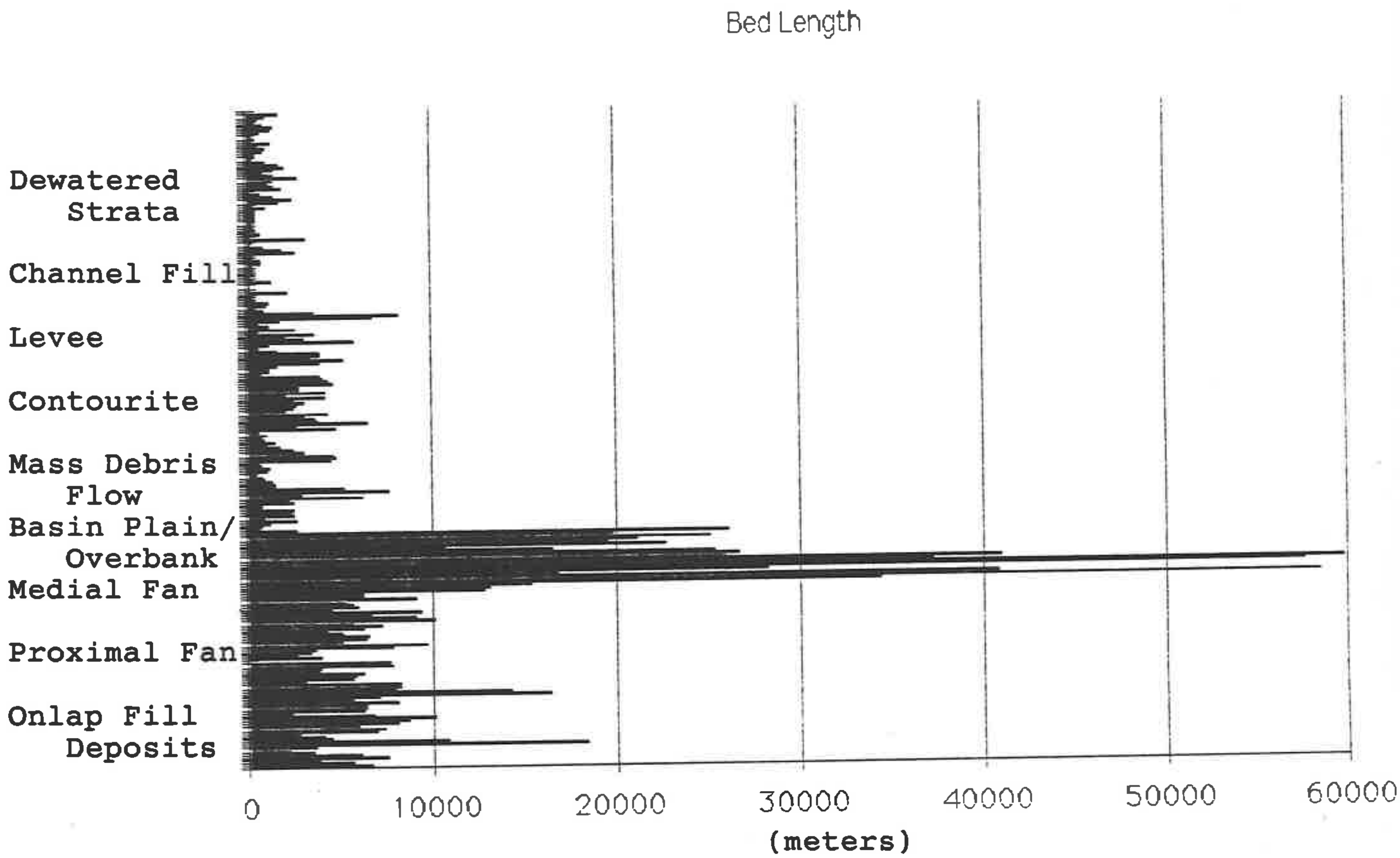

Bed Length
Dewatered Strata
Channel Fill
Levee
Contourite
Mass Debris Flow
Basin Plain/ Overbank
Medial Fan
Proximal Fan
Onlap Fill Deposits
0
10000
20000
30000
40000
50000
60000
(meters)

Figure 16

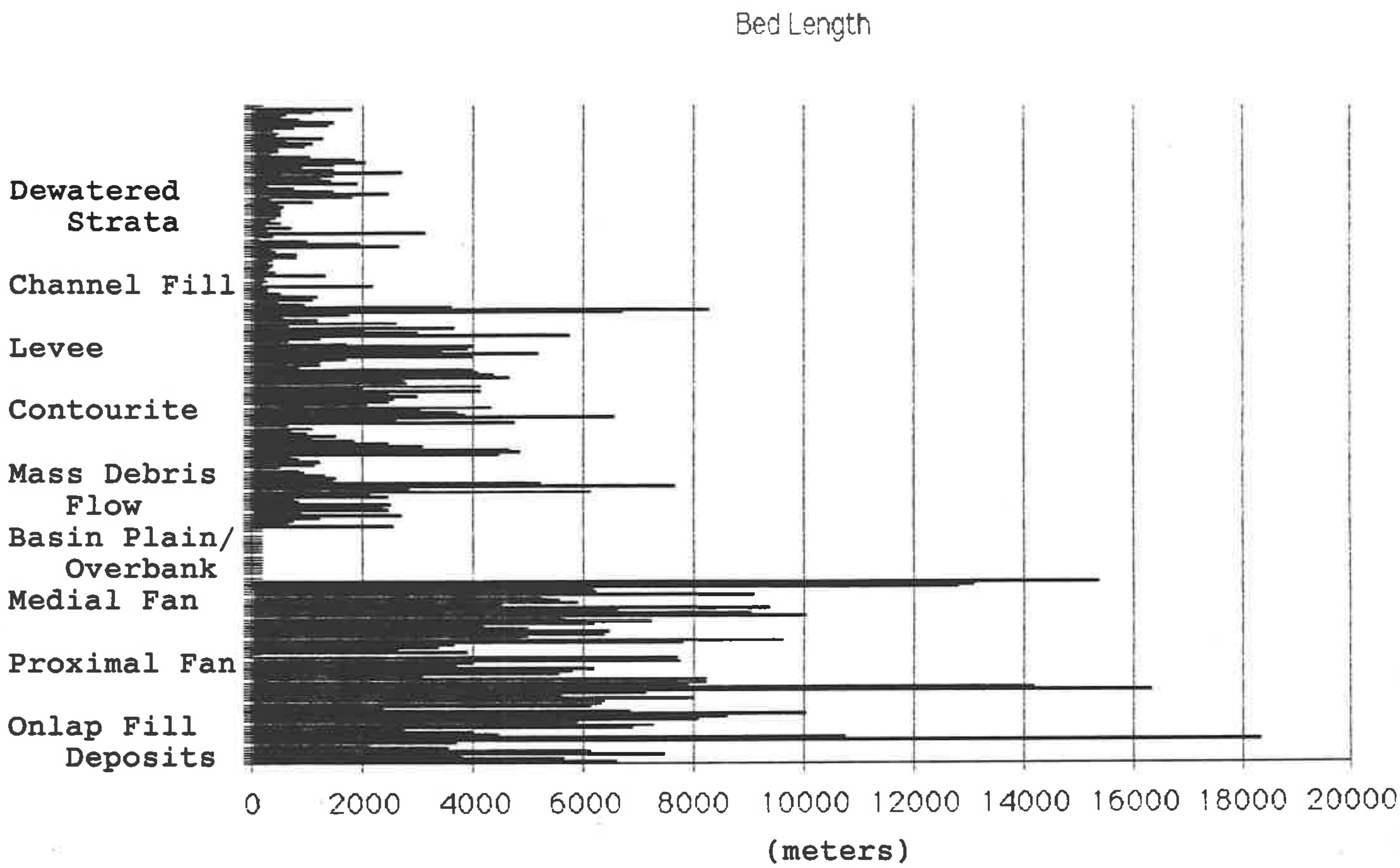
Bed Length
Dewatered Strata
Channel Fill
Levee
Contourite
Mass Debris Flow
Basin Plain/ Overbank
Medial Fan
Proximal Fan
Onlap Fill Deposits
0
2000
4000
6000
8000
10000
12000
14000
16000
18000
20000
(meters)

<u>Figure 17</u>